

# Resonance Raman Scattering with Continuum of Nonbonded States on the Example of Aluminium Dimer

(Project in the Dept. of Theoretical Chemistry on the Jagiellonian University)

author: Mariusz Radoń

supervisor and tutor: Prof. dr hab. Marek T. Pawlikowski

Cracow 2005 (revised 2006)

## Abstract

Aluminium dimer ( $\text{Al}_2$ ) is being suspected of having non-bonding (dissociative) excited electronic state ( $1^3\Pi_g$ ), dipole-connected to the ground state. The continuum of nuclear non-bonded states in the manifold of this non-bonding electronic state may be therefore crucial for the understanding of resonance Raman (RR) spectrum of  $\text{Al}_2$ , which was recently obtained in solid argon matrix by Fang *et al.*[1].

So called *reflection approximation*[2] was proposed in the literature for the case of resonance with continuum, but due to its limitation here we introduce more realistic approximation, which leads to equations that can be easily solved numerically. Potential energy curves for interesting electronic states, needed as input for the proposed method, have been obtained using Complete Active Space calculations (CASSCF-PT2). This multiconfigurational approach, in combination with Density Functional calculations, was also used to study electronic structure of low-lying states of  $\text{Al}_2$  and to obtain basic spectroscopic constants. These results are compared with experimental data and theoretical results due to Bauschlicher, Langhoff *et al.*[3, 4].

## 1 Electronic structure and spectroscopic constants

### 1.1 Methods

Complete active space self consistent field method, (CASSCF[5]) followed by second-order multiconfigurational perturbation theory (CASPT2[6]) calculations have been performed using Molcas package[7]. Below we refer to this method as CASSCF-PT2. The Correlation Consistent Polarized Valence Triple and Quadruple Zeta (cc-pVTZ and cc-pVQZ) basis sets[8] were used. Calculations were performed in  $D_{2h}$  symmetry group (the highest supported by Molcas suite), with molecule lying on  $z$  axis. The active space used was composed of valence orbitals only (i.e. those arising from 3s and 3p shells of Al), however

in case of cc-pVQZ it was increased with three additional orbitals (the lowest of  $b_{2u}$ ,  $b_{3u}$  and  $b_{2g}$  symmetries) to solve intruder state problem for  $1^3\Sigma_u^-$  state. Electronic transition dipole moments (TDMs) were computed from CASSCF wavefunctions as a function of distance.

Density Functional Theory (DFT) calculations in spin-unrestricted version have been performed with Amsterdam Density Functional (ADF) [9, 10, 11] program for states  $1^3\Pi_u$ ,  $1^3\Sigma_g^-$  and  $1^3\Pi_g$ , which states can be well represented by single Slater determinant (this assumption was further supported by CASSCF results). The calculations took place in standard TZ2P Slater Type Orbitals basis set of ADF with the following exchange-correlation functionals: Local Spin Density Approximation (LSDA) (in VWN[12] parametrization with Stoll's correction[13]), PW91[14] and BLYP[15, 16, 17, 18].

## 1.2 Results and discussion

Figures 1 and 2 show potential energy curves from example DFT and CASSCF-PT2 calculations. Spectral properties of  $1^3\Pi_u$  and  $1^3\Sigma_g^-$  electronic states – the equilib-

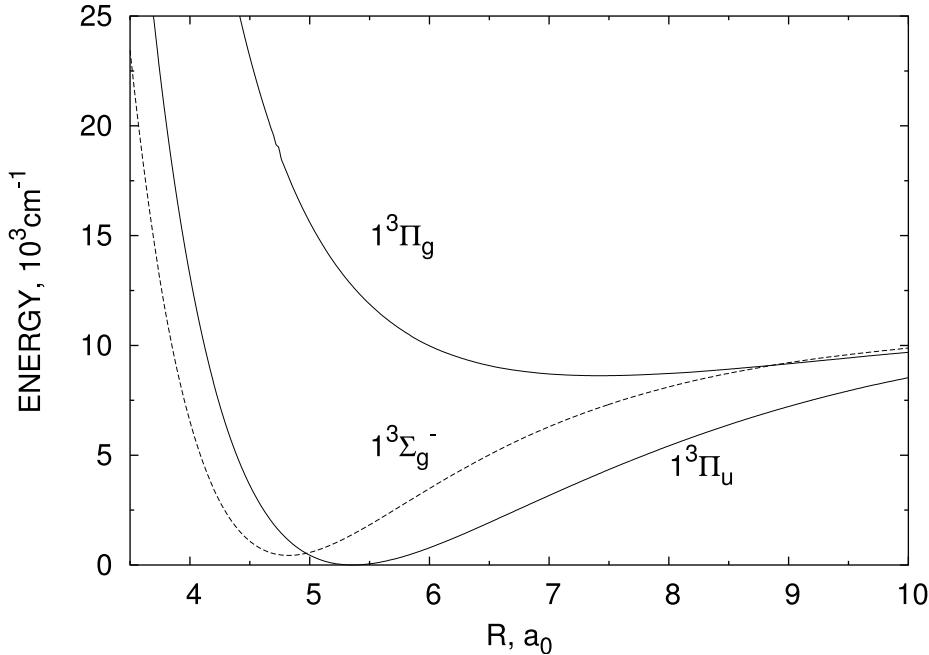


Figure 1: Potential energy curves for selected low lying states of  $\text{Al}_2$  from DFT calculations with BLYP functional

rium bondlength ( $R_e$ ), equilibrium frequency ( $\omega_e$ ), anharmonicity ( $\omega_a x_e$ )<sup>1</sup> and vibrational ground state energy ( $G_0$ ) – are presented in tables 1, 2. The last table contains also the adiabatic difference in energy between  $1^3\Sigma_g^-$  and  $1^3\Pi_u$  ( $T_0$ ). The vertical energies (plus

---

<sup>1</sup>Equilibrium frequency and anharmonicity coefficient come from *numerically* obtained energies of vibrational terms by fitting them with the Morse formula

$$E_v = \hbar\omega_e\left(v + \frac{1}{2}\right)\left(1 - x_e\left(v + \frac{1}{2}\right)\right)$$

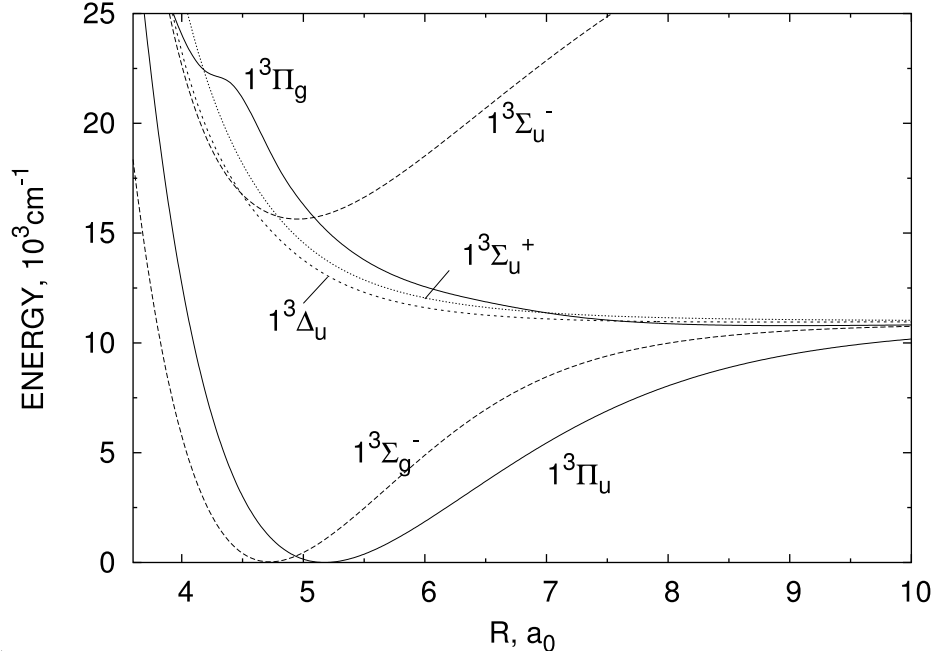


Figure 2: Potential energy curves for low lying states of  $\text{Al}_2$  from CASSCF-PT2 calculations using cc-pVTZ basis set

TDMs for dipole-allowed transitions) for equilibrium geometries of  $1^3\Pi_u$  and  $1^3\Sigma_g^-$  are given in tables 4, 5. Approximated bonding energy ( $\epsilon$ ) and equilibrium bondlength ( $R_e$ ) for nearly non-bonding  $1^3\Pi_g$  state are given in table 3, however they are much less accurate, because were obtained just by approximating potential energy curve for the considered state with Lennard-Jones potential with exponent providing the best fit.

Method	Basis set / functional type	$R_e$ Å	$\omega_e$ $\text{cm}^{-1}$	$\omega_e x_e$ $\text{cm}^{-1}$	$G_0$ $\text{cm}^{-1}$
KS-DFT	LDA	2.754	253.2	1.39	126.6
	PW91	2.836	221.3	1.32	110.9
	BLYP	2.746	251.0	1.51	125.7
CASSCF-PT2	cc-pVTZ	2.737	279.0	1.51	139.2
	cc-pVQZ	2.725	280.7	1.53	140.0
MR-CI[4]	ANO-L	2.835	274	—	—
Exp.[1]	—	—	295.7(5)	1.68(5)	—

Table 1: Spectral data for  $1^3\Pi_u$  state of  $\text{Al}_2$

Some conclusions can be drawn:

- DFT and CASSCF-PT2 curves are similar except from the region of avoided crossing of  $1^3\Pi_g$  with  $2^3\Pi_g$  (not discussed in this paper, see [4]) which reflects in characteristic shape of CASSCF-PT2 curve for  $1^3\Pi_g$ , unlike DFT one.

Method	Basis set / functional type	$T_0$ $\text{cm}^{-1}$	$R_e$ $\text{\AA}$	$\omega_e$ $\text{cm}^{-1}$	$\omega_e x_e$ $\text{cm}^{-1}$	$G_0$ $\text{cm}^{-1}$
KS-DFT	LDA	-593.1	2.488	335.0	2.03	167.0
	PW91	437.2	2.554	294.7	2.37	146.8
	BLYP	551.5	2.493	323.4	2.35	161.2
CASSCF-PT2	cc-pVTZ	28.6	2.502	345.6	2.06	172.4
	cc-pVQZ	4.39	2.491	347.0	2.07	172.9
MR-CI [4]	ANO-L	227	2.496	331	–	–

Table 2: Spectral data for  $1^3\Sigma_g^-$  state of  $\text{Al}_2$

Method	Basis set / functional type	$R_e$ $\text{\AA}$	$\epsilon$ $10^3\text{cm}^{-1}$
KS-DFT	LDA	3.62	4.78
	PW91	3.93	3.27
	BLYP	3.68	3.72
CASSCF-PT2	cc-pVTZ	4.74	0.25
	cc-pVQZ	4.46	0.30

Table 3: Spectral data for  $1^3\Pi_g$  state of  $\text{Al}_2$

Method	Basis set / functional type	Vertical energies (and TDMs) $10^3\text{cm}^{-1}(\text{a.u.})$						
		$1^3\Sigma_g^-$	$1^3\Delta_u$	$1^3\Sigma_u^+$	$1^3\Pi_g$	$1^3\Sigma_u^-$		
KS-DFT	LDA	0.553	(–)	–	–	14.269	(–)	–
	PW91	1.388	(–)	–	–	12.706	(–)	–
	BLYP	1.514	(–)	–	–	13.926	(–)	–
CASSCF-PT2	cc-pVTZ	1.032	(0.166)	13.139	13.826	15.216	(0.789)	15.828
	cc-pVQZ	0.992	(0.258)	13.330	14.037	14.814	(0.681)	16.255

Table 4: Vertical energies (and TDMs for dipole connected states) measured from  $1^3\Pi_u$  state of  $\text{Al}_2$  at its equilibrium geometry

- Except from LSDA  $1^3\Pi_u$  is always predicted as a ground state, which is in agreement with [4]. However the adiabatic energy distance between two lowest states –  $1^3\Pi_u$  and  $1^3\Sigma_g^-$  – changes very much from one method another. Our CASSCF-PT2 results in both basis sets give this parameter much smaller (28.6 and 4.39  $\text{cm}^{-1}$ ) than 227  $\text{cm}^{-1}$  reported in [4]. However, there is a relatively big difference in vibrational ground state energies between  $1^3\Pi_u$  and  $1^3\Sigma_g^-$  (at least 60  $\text{cm}^{-1}$  more for  $1^3\Sigma_g^-$ , according to our results) so *even if electronic states were degenerated at*

Method	Basis set / functional type	Vertical energies (and TDMs) 10 <sup>3</sup> cm <sup>-1</sup> (a.u.)						
		1 <sup>3</sup> Π <sub>u</sub>		1 <sup>3</sup> Δ <sub>u</sub>		1 <sup>3</sup> Σ <sub>u</sub> <sup>-</sup>		1 <sup>3</sup> Σ <sub>u</sub> <sup>+</sup>
KS-DFT	LDA	1.845	(-)	-	-	(-)	-	20.143
	PW91	0.683	(-)	-	-	(-)	-	17.239
	BLYP	0.559	(-)	-	-	(-)	-	18.429
CASSCF-PT2	cc-pVTZ	1.121	(0.226)	15.121	15.855	(0.422)	16.164	18.630
	cc-pVQZ	1.124	(0.321)	15.426	16.421	(0.638)	16.484	17.981

Table 5: Vertical energies (and TDMs for dipole connected states) measured from 1<sup>3</sup>Σ<sub>g</sub><sup>-</sup> state of Al<sub>2</sub> at its equilibrium geometry

*their minima the ground vibronic term for 1<sup>3</sup>Π<sub>u</sub> would be still a ground state term<sup>2</sup>.*

- 1<sup>3</sup>Π<sub>g</sub> state is slightly bonding in all calculations performed (this may be the artifact of gaussian basis or of not including basis set superposition error). Its eventual bonded states are probably not important for RR spectroscopy of Al<sub>2</sub>, however their small contribution to RR amplitude was included.
- The experimental ground state equilibrium frequency 295.7 cm<sup>-1</sup> is reproduced quite well. Comparison of our value with other theoretical works (rather good agreement) suggest the difference is probably due to influence of solid argon matrix, just like the site effect (splitting of the lines in RR spectrum) reported in [1].

## 2 Resonance Raman scattering spectrum

### 2.1 Introduction – theory of resonance Raman scattering

Standard expression for the scattering tensor for transition between states *i* (*initial*) and *f* (*final*) is as follows:

$$\alpha_{\rho\sigma}^{i\rightarrow f} = \sum_n \frac{(\langle \Psi_f | d_\rho | \Psi_n \rangle)(\langle \Psi_n | d_\sigma | \Psi_i \rangle)}{E_n - E_i - \hbar\Omega - i\Gamma_n} + \sum_n \frac{(\langle \Psi_f | d_\sigma | \Psi_n \rangle)(\langle \Psi_n | d_\rho | \Psi_i \rangle)}{E_n - E_f + \hbar\Omega - i\Gamma_n} \quad (1)$$

where  $\Psi_i, \Psi_f$  are the wavefunctions of the proper vibronic states,  $E_i, E_f$  – their energies,  $\Omega$  – the frequency of incident light.  $\langle \rangle$  is the inner product in  $N$ -electron Hilbert space and  $()$  is the inner product in nuclear space. The sums (integrals in case of continuum) are over all *intermediate states*  $\Psi_n$ , each of energy  $E_n$  and decay rate (i.e. inverse of the

<sup>2</sup>Assuming the mentioned difference in vibrational ground state energies equals 60 cm<sup>-1</sup>, only about 10% of molecules should occupy 1<sup>3</sup>Σ<sub>g</sub><sup>-</sup> state in the temperature of experiment [1] (less than 40 K).

lifetime)  $\Gamma_n$ . Intensities of Raman transitions are proportional to sum of squares of the above amplitudes

$$I_{\text{tot}}^{i \rightarrow f} \propto \Omega^4 \sum_{\rho, \sigma} |\alpha_{\rho\sigma}|^2 \quad (2)$$

In the case of resonance Raman (RR) scattering the second (so called *antiresonance*) sum in (1) may be neglected and the remaining first term is dominated by the contribution from the manifold of one particular electronic state, i.e. the one being in resonance with incidenting light.

For  $\text{Al}_2$  there are two channels of resonance scattering theoretically possible in the range of laser frequency used in the experiment[1]:  $1^3\Sigma_g^- \rightarrow 1^3\Sigma_u^- \rightarrow 1^3\Sigma_g^-$  (resonance with bonded states) and  $1^3\Pi_u \rightarrow 1^3\Pi_g \rightarrow 1^3\Pi_u$  (resonance with continuum). In this second channel the sum should be replaced with the integral. For considered transitions we have only one non-zero component of scattering tensor, i.e.  $\alpha_{zz} \equiv \alpha$ . Final formula for  $\alpha$  is

$$\alpha = \int_D^\infty dE \rho(E) \frac{(\psi_f | d | \phi_E)(\phi_E | d | \psi_i)}{E - E_i - \hbar\Omega - i\Gamma_E} \quad (3)$$

where  $\phi_E$  is a nuclear wavefunction of non-bonded state of energy  $E$ ,  $\rho(E)$  is the energetical density of nuclear states (density of states, DOS) and  $d$  is the  $z$  component of transition dipole moment between electronic states  $1^3\Pi_u$  and  $1^3\Pi_g$ .

Decay rate  $\Gamma_E$  in the mentioned experiment seems to have main contributions from:

- radiative decay to  $1^3\Pi_u$  manifold (can be roughly estimated on  $\simeq 10^{-4}$ - $10^{-3}\text{cm}^{-1}$ )
- radiationless decay (should not be very important because non-adiabatic coupling elements are non-zero only for  $1^3\Pi_g$  and  $1^3\Pi_u$ , which states are well separated)
- radiationless transfer of the energy to solid matrix

The last contribution (from the solid matrix) is probably the most important, but unfortunately it cannot be predicted at all on the basis of single molecule model considered here. Thus, for simplicity we assume that  $\Gamma_E \equiv \Gamma$  *does not depend on the energy*, so is treated as an *parameter*. Then RR spectrum will be computed for various values of  $\Gamma$  to analyse its influence.

## 2.2 Nuclear states for bonding and non-bonding potentials

To compute  $\alpha$  from (3) one need to have nuclear wavefunction in either analytical or numerical form, especially in the Franck-Condon region of the ground state (due to the integration with ground state vibrational wavefunctions, localized mainly in this region). To obtain these functions for diatomic molecule in Born-Oppenheimer approximation one has to solve the radial Schrödinger equation:

$$-\frac{\hbar^2}{2\mu} \frac{d^2\psi}{dr^2} + V(r)\psi(r) = E\psi(r) \quad (4)$$

where  $\mu$  is the reduced mass of molecule. There are standard numerical algorithms of solving (4) for bonded nuclear states, but *not for the continuum* of non-bonded (scattering) states.

Unfortunately, the pretty formalism of scattering theory cannot be applied here, due to the reason that it is useful in predicting wavefunction *far from the molecule*, in principle in the infinity, but not in the Franck-Condon region, where the nuclear wavefunctions are needed.

So called *reflection approximation*[2] was proposed for the case of resonance with continuum. In this approximation the repulsive potential is modelled as decreasing, linear function of nuclear coordinate *very steep, so much that the solution of (4) may be approximated as Dirac delta* centered in the turning point of the classical particle possessing the given energy. Furthermore, it is assumed that  $\Gamma \rightarrow 0$  (long-living states) and transition dipole moment (TDM) does not depend on the coordinate  $r$ . Though this model provides analytical solutions, its physical foundations are arbitrary; it is also non sensitive to any details of repulsive nuclear potential and does not include dependence of TDM on  $r$ . Due to these reasons reflection approximation may seem to be rather *qualitative* than *quantitative* model of RR. Therefore there is a need for more realistic, numerical model. No matter how useful it will be in every-day routine interpretation of RR spectra for typical molecules, it can be extremely interesting to compare its predictions with the results of reflection approximation (at least for few model systems).

The main problem with solving (4) numerically for non-bonded states concerns the *boundary conditions*. For bonded state wavefunction  $\psi$  it is true that

$$\psi(r \rightarrow 0) = 0 \quad (5)$$

$$\psi(r \rightarrow \infty) = 0 \quad (6)$$

because of faster than exponential decay of  $\psi$  in growing, repulsive potential. In practise one is interested in solving (4) in the interval  $\{r : 0 < a \leq r \leq b < \infty\}$  (“the box”), and conditions (5) and (6) are assumed to hold on the edges of the “box”

$$\psi(a) = 0 = \psi(b) \quad (7)$$

provided that it is sufficiently large (i.e.  $a \approx 0$  and  $b$  is big enough in comparison with the size of Franck-Condon region). Then, equation (4) can be easily solved numerically, e.g. on the one-dimensional grid (see below).

For non-bonded state only the first boundary condition (at zero) holds – but no such condition is true in the infinity, where the wavefunction has plane-wave type asymptotic behaviour. One may ask *what happen when one enforce the second condition also, i.e. put  $\psi(b) = 0$ , where  $b$  is large*. From the asymptotic behaviour of solutions ( $\sim e^{ikr} + \lambda e^{-ikr}$ ) one can realize that this requirements simply *selects a discrete subset of states form the continuum*. Moreover from the same asymptotic behaviour it turns out that, for  $b$  large enough there exist states (satisfying  $\psi(b) = 0$ ) *of energy as close as is needed to any value in the continuum*. The idea of the proposed method is therefore to solve (4) on  $[a : b]$  under conditions (7) *in the same way as for bonded states*, obtaining a discrete subset of solutions as a result. The “box”  $[a : b]$  should be sufficiently large to get rid of artifacts arising from its finite size. Then, any property of the continuum being the smooth function (e.g. density of states, transition dipole moment) which can be computed for the found discrete set of solutions can be *interpolated* over continuum, which makes possible to evaluate integrals such like (3).<sup>3</sup>

---

<sup>3</sup>There is one caveat in this reasoning: the method holds only for the case of non-degenerated

In our approach the discrete and continuous part of the spectrum are treated equally. However, during the summation/integration these two types of solutions should be distinguished: *integration is only over states above dissociation limit*. To find the estimate of the dissociation limit consistent with the character of solutions found in particular, finite “box” we employed the criterion of the *maximum density of states*: for energies above this critical value one has “continuum”, and below one has “bonded states” (in purely operational sense). Of course our method leads to poor description of states nearest to the dissociation limit and these states can be erroneously classified as “bonded states” or “continuum”. From these reasons if these states give important contribution to any property one would probably experience strong dependence of final results on the “box” size, especially on  $b$ . In such cases the proposed method should be used with *very large* “boxes” or even may be not applicable. However, this is not the case of the system being studied here, as our numerical tests showed.

Equation (4) was solved using the standard grid techniques for the one-dimensional Schrödinger equation. The radial wavefunction  $\psi(r)$  was discretized onto a thick grid of points  $\{r_0 \equiv a, r_1, \dots, r_n, r_{n+1} \equiv b\}$ ,  $r_{i+1} = r_i + s$  as an array  $\boldsymbol{\psi} = \{\psi_i \equiv \psi(r_i)\}$ . The second derivative in (4) was approximated by finite difference, three point approximation [19]. Adding boundary conditions (5, 6) we reduce (4) to algebraic eigenproblem (with tridiagonal matrix)

$$\tilde{H}\boldsymbol{\psi} = \epsilon\boldsymbol{\psi} \quad (8)$$

where  $\tilde{H} = \text{trid}((-1, \dots, -1); (2 + u_1, \dots, 2 + u_n); (-1, \dots, -1))$ ,  $u_i = 2ms^2V(r_i)/\hbar$ ,  $\epsilon = 2ms^2E/\hbar$ , which is therefore solved numerically.

The final computed amplitudes are checked to be stable in respect to increasing the interval  $[a : b]$  and the upper limit of integration in (3).

## 2.3 Results

Predicted RR spectra for  $1^3\Pi_u \rightarrow 1^3\Pi_g \rightarrow 1^3\Pi_u$  channel of scattering for variety of  $\Gamma$  values are shown in figure 3 (the wavelength of incident laser light is 660 nm, like in exp. [1]). Our results are compared with the predictions from the reflection approximation (RA). In the limit of  $\Gamma \rightarrow 0$  (as in RA) the progression is *extremely long* but not similar to progression from RA. But since one neglects the dependence of TDM on nuclear coordinate (i.e. replaces integrals with TDM by nuclear wavefunctions overlap integrals),

---

continuum, or continuum having at least *countable* subset of degenerated solutions (the simplest example of degenerated continuum is free-particle problem in one dimension – for *any* value of energy there are two solutions – e.g.  $\sin(kx)$ ,  $\cos(kx)$ ). The reason of the failure in case of degeneracy is that for the degenerated values of the energy the method *recovers only one of few degenerated states* (even in the limit of infinitely large “box”!). However, if the degeneracy is restricted only to countable (either finite or infinite) subset of energies these values of energy can be safely removed from the integration domain in (3) without any change of results (because they form a set of zero measure by our assumption). In this way isolated (“random”) degenerations in the spectrum are acceptable for the method and the only requirement is that the spectrum cannot be *systematically* degenerated. This type of degeneration usually (if not always) comes from symmetry (e.g. in the case of free particle it is due to spatial inversion symmetry). We do not expect, however, any type of systematic degeneracy for typical repulsive energy curves, since they have no such symmetry. However, we cannot make formal proof of this fact and can only conclude once again that systematic degeneracy is extremely unexpected due to lack of any spatial symmetry in potential function  $V(r)$ .



as RA assumes, both progressions are more similar to each other in the limit of  $\Gamma \rightarrow 0$  (see figure 4). For comparison purposes the analogous simulation has been done for the second

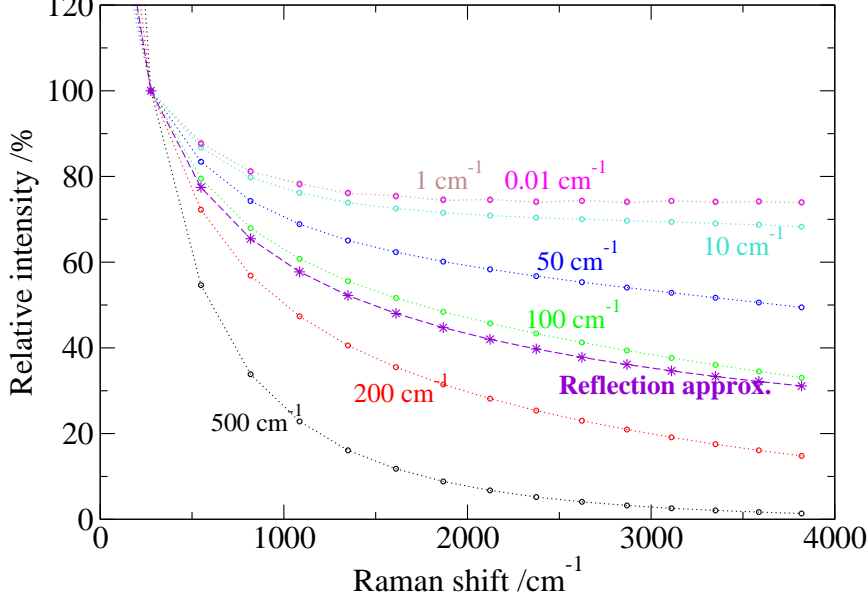


Figure 3: Predicted spectra for the channel  $1^3\Pi_u \rightarrow 1^3\Pi_g \rightarrow 1^3\Pi_u$  for variety of  $\Gamma$  values (Raman resonance with continuum). The incident wavelength is 660 nm

possible channel of scattering  $1^3\Sigma_g^- \rightarrow 1^3\Sigma_u^- \rightarrow 1^3\Sigma_g^-$  (only bonded states as intermediates). At laser wavelength 660 nm (like in exp. [1]) we observe preresonance Raman effect (short progression, only slight dependence on  $\Gamma$ , figure 5). If the wavelength is  $\simeq 642$  nm the resonance with first bonded state in  $1^3\Sigma_u^-$  manifold occurs (illustrated in figure 6).

## 2.4 Conclusions

The proposed method of solving radial Schrödinger equation for non-bonded states proved to be feasible and stable enough to obtain results for diatomic system ( $\text{Al}_2$ ). Its results are different from the reflection approximation even in the limit of  $\Gamma \rightarrow 0$ , however the difference in this limit seems to be mainly due to the fact that real transition moment depend on the nuclear coordinate.

Unfortunately, the computed Raman spectra cannot be directly compared with experimental data, since  $\Gamma$  is unknown.  $\Gamma$  may be estimated by comparison of computed and observed spectral progression. In this way one can find that  $\Gamma$  should be *very large*, about  $10^2 \text{ cm}^{-1}$  to make agreement with experimental spectrum. This large value can be understood as an effect of the strong interaction with the matrix. On the other hand, in the case of such strong interaction one can doubt that description by continuum is good for  $\text{Al}_2$  imprisoned in the matrix. However, we do not even try to predict the spectrum for such complicated situation.

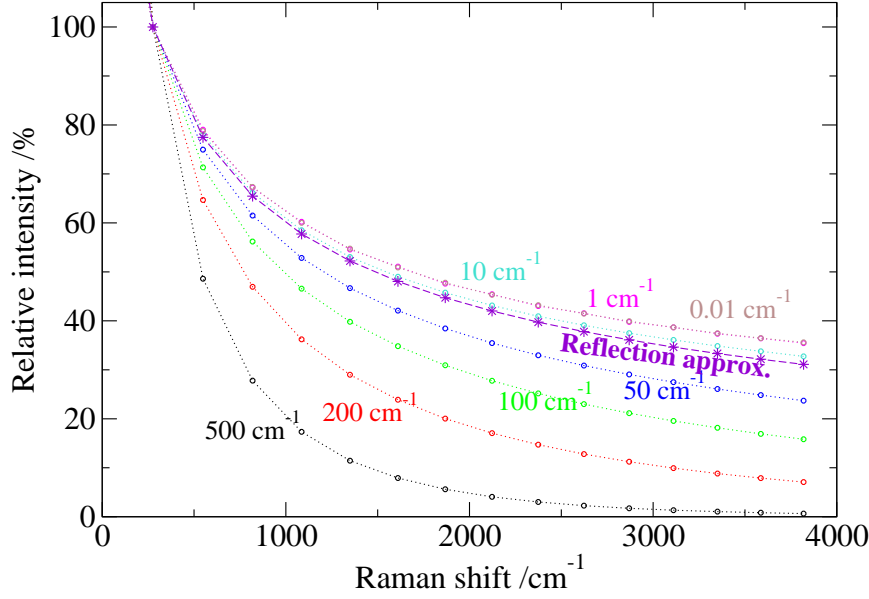


Figure 4: Predicted spectra for the channel  $1^3\Pi_u \rightarrow 1^3\Pi_g \rightarrow 1^3\Pi_u$  for variety of  $\Gamma$  values calculated under assumption that TDM does not depend on nuclear coordinate. The incident wavelength is 660 nm.

However, in gas phase  $\Gamma$  may be very small (due to the lack of the solid matrix) and we expect *quite long progression* (see figure 3). Progression may be longer than reflection approximation predicts (if only  $\Gamma$  can be reduced to the order of  $10^1 \text{ cm}^{-1}$ ; due to our rough estimations internal contributions to *Gamma* – spontaneous emission + vibronic interaction + dissociation – are much smaller). It would be very interesting to verify this prediction experimentally, but as authors know no experimental RR spectra of  $\text{Al}_2$  in the gas phase exists yet.

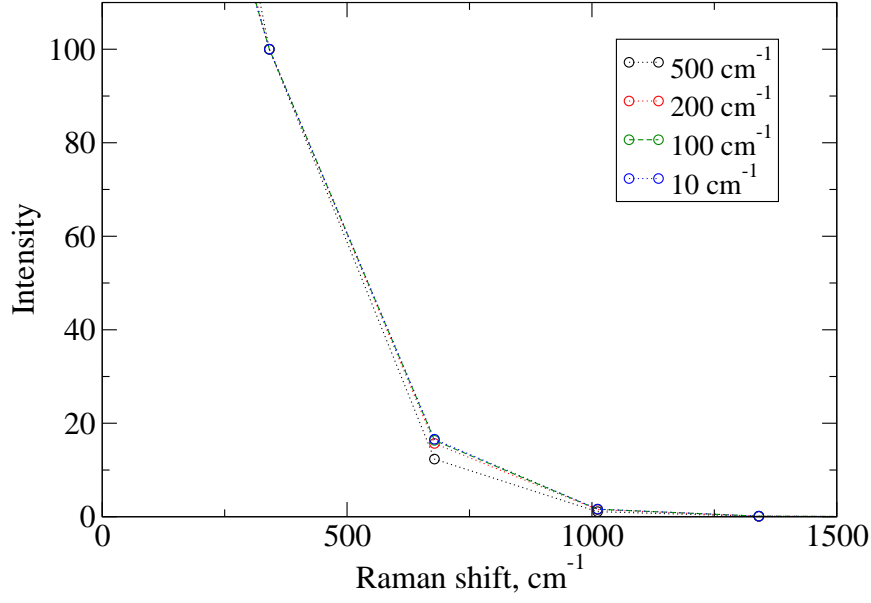


Figure 5: Predicted spectra for the channel  $1^3\Sigma_g^- \rightarrow 1^3\Sigma_u^- \rightarrow 1^3\Sigma_g^-$  for variety of  $\Gamma$  values (preresonance Raman effect). The incident wavelength is 660 nm.

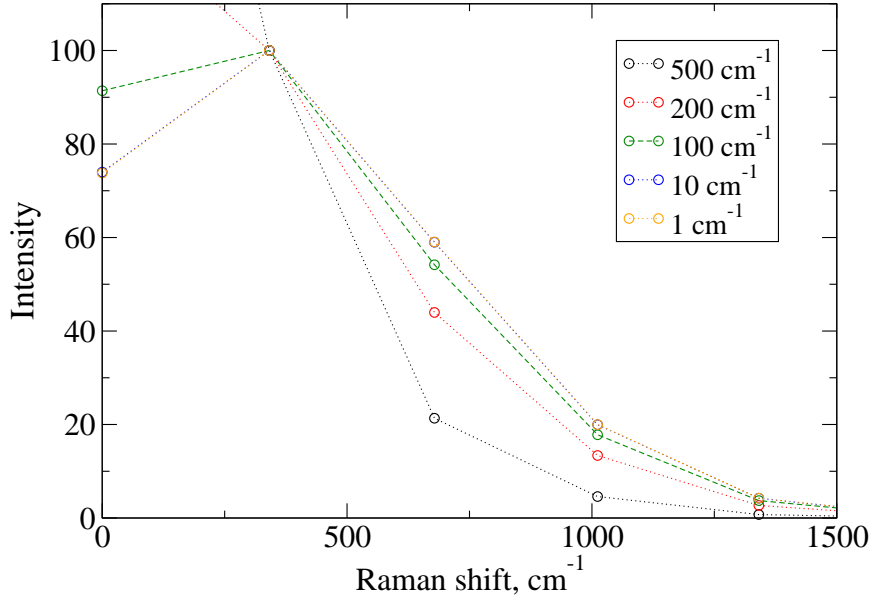


Figure 6: Predicted spectra for the channel  $1^3\Sigma_g^- \rightarrow 1^3\Sigma_u^- \rightarrow 1^3\Sigma_g^-$  for variety of  $\Gamma$  values (Raman resonance with bonding state). The incident wavelength is 642 nm.

## References

- [1] L. Fang, B. L. Davis, H. Lu, and J. R. Lombardi, *Spectrochimica Acta Part A* **57**, 2809 (2001).
- [2] M. Mingardi and W. Siebrand, *Chemical Physics Letters* **23**, 1 (1973).
- [3] J. Charles W. Bauschlicher and S. R. Langhoff, *Journal of Chemical Physics* **90**, 4627 (1989).
- [4] S. R. Langhoff and C. W. Bauschlicher, *Journal of Chemical Physics* **92**, 1879 (1990).
- [5] B. O. Roos, P. R. Taylor, and P. E. M. Siegbahn, *Chemical Physics* **48**, 157 (1980).
- [6] K. Andersson, P. Malmqvist, B. Roos, A. Sadlej, and K. Wolinski, *Journal of Physical Chemistry* **94**, 5483 (1990).
- [7] K. Andersson *et al.*, *MOLCAS Version 5.4* (Dept. of Theor. Chem., Chem. Center, Univ. of Lund, P.O.B. 124, S-221 00 Lund, Sweden, 2002).
- [8] D. Woon and T. Dunning Jr., *Journal of Chemical Physics* **98**, 1358 (1993).
- [9] G. t. Velde *et al.*, *Journal of Computational Chemistry* **22**, 931 (2001).
- [10] C. Fonseca Guerra, J. Snijders, G. t. Velde, and E. Baerends, *Theoretical Chemistry Accounts* **99**, 391 (1998).
- [11] E. J. Baerends *et al.*, *Amsterdam Density Functional (ADF) ver. 2002.03* (SCM, Theoretical Chemistry, Vrije Universiteit, <http://www.scm.com>, 2002).
- [12] S. Vosko, L. Wilk, and M. Nusair, *Canadian Journal of Physics* **58**, 1200 (1980).
- [13] H. Stoll, C. Pavlidou, and H. Preuss, *Theoretica Chimica Acta* **49**, 143 (1978).
- [14] J. Perdew *et al.*, *Physical Review B* **46**, 6671 (1992).
- [15] A. Becke, *Physical Review A* **38**, 3098 (1988).
- [16] C. Lee, W. Yang, and R. Parr, *Physical Review B* **37**, 785 (1988).
- [17] B. Johnson, P. Gill, and J. Pople, *Journal of Chemical Physics* **98**, 5612 (1993).
- [18] T. Russo, R. Martin, and P. Hay, *Journal of Chemical Physics* **101**, 7729 (1994).
- [19] C. Gerald and P. Wheatley, *Applied Numerical Analysis* (Addison-Wesley, Reading, 1989).